

## Identification of the Near-Infrared Absorption Band from the Mn Cluster of Photosystem II

Richard Baxter,<sup>‡</sup> Elmarz Krausz,<sup>§</sup> Tom Wydrzynski,<sup>||</sup> and Ron J. Pace\*<sup>‡</sup>

Research School of Biological Sciences  
Research School of Chemistry  
and Department of Chemistry, Faculty of Science  
Australian National University, Canberra 0200, Australia

Received November 9, 1998  
Revised Manuscript Received April 21, 1999

The site for water oxidation in photosystem II (PS II)<sup>1</sup> of higher plants and algae is a cluster of four Mn ions, called the oxygen evolving complex (OEC).<sup>2</sup> EXAFS data indicate that the OEC contains a pair of  $\mu$ -oxo bridged Mn dimers,<sup>3</sup> the extent of exchange mediated interaction between these dimers being currently the subject of debate (e.g. refs 3 and 4). Oxidation of water involves passage through four quasistable intermediate oxidation states of the OEC, called S states (labeled S<sub>0</sub>...S<sub>3</sub>).<sup>2</sup> S state advancement occurs through single photon turnover and involves Mn oxidation on at least some steps. The system relaxes to the S<sub>1</sub> state on dark incubation.

Strong optical absorptions by chlorophyll ( $\lambda < 700$  nm) and solvent water ( $\lambda > 1000$  nm) define a near-infrared (NIR) window between  $\sim 750$  and 1000 nm in PS II. High-valent Mn is known to have weak absorption bands in this region.<sup>5</sup> In 1984 Dismukes and Mathis<sup>6</sup> reported a low-intensity NIR band in PS II particles that was attributed to the S<sub>2</sub> state. This band was relatively featureless in the range 730–900 nm, with a peak around 750 nm. In 1988 Velthuys<sup>7</sup> was unable to repeat this result and attributed the earlier observations to S state dependent scattering effects. However, Boussac et al. have recently shown<sup>8</sup> low-temperature (<150 K) interconversion of Mn-derived S<sub>2</sub> state EPR signals in PS II (the so-called multiline and *g* 4.1 resonances<sup>2</sup>), by exposure to continuous near-infrared illumination. The action spectrum for this effect was distinct from the earlier claimed band-(s) and showed a resolved maximum at  $\sim 820$  nm. Here we report the first observation of a NIR absorption band in the S<sub>2</sub> state of PS II that closely matches the action spectrum of the NIR induced spin state interconversion. This study employed solubilized PS II core complexes (to enhance the OEC-to-chlorophyll ratio and reduce scattering) and a high performance single beam absorption

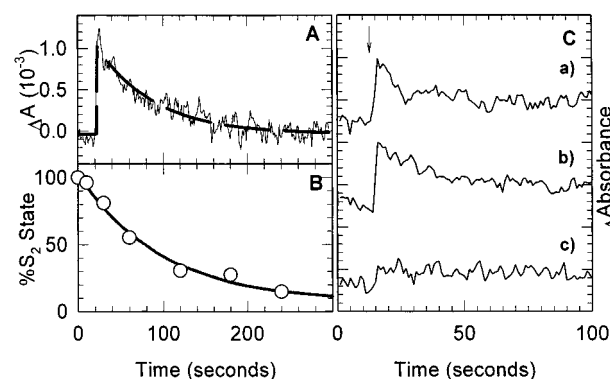


**Figure 1.** (A) Turnover–decay kinetics of NIR signal at 820 nm and 2 °C following flash (arrow) on dark-adapted (S<sub>1</sub> state) PS II core particles (1 mg/mL Chl). Average of 12 transients. The dashed line is the fitted single-exponential decay ( $t_{1/2} = 50$  s). (B) S<sub>2</sub> state decay kinetics of material in part A observed by oxygen flash yield measurements on a Joliot electrode (ref 11). The temperature was in the range 0–2 °C on the electrode. The solid line is the single-exponential decay fit ( $t_{1/2} = 65$  s). (C) Effects of reagent additions on NIR signal turnover: (a) control, (b) plus 2% (v/v) MeOH, and (c) + 5 mM hydroxylamine. Other conditions as in part A.

apparatus, able to detect  $\Delta A$  changes of  $10^{-5}$  in a 1 Hz bandwidth.<sup>9</sup> Repetitive turnover from S<sub>1</sub> to S<sub>2</sub> (with dark relaxation) was used as S state coherence is quickly lost with multiple turnover of core particles.<sup>10</sup>

PS II particles and core complexes were prepared by standard methods.<sup>11,12a</sup> After elution from the FPLC column, the core samples were concentrated in Centricon 3 ultrafiltration cartridges (Amicon) to a concentration of 1–2 mg chl/mL. The material had a chlorophyll a/b ratio >20 and a steady-state O<sub>2</sub> activity of 1600–2000  $\mu$ mol O<sub>2</sub>/mg chl per h. NIR measurements were performed on a purpose built single beam apparatus,<sup>9</sup> with saturating single turnover flashes generated from a Nd:YAG laser. The measurement cuvette had path lengths of 1 cm (measurement) and 2 mm (illumination) and spectra were acquired at 2 °C, with [chl] = 1 mg/mL in the elution buffer.<sup>12a</sup> Turnover flash spacing was 250 s, which permits essentially complete S<sub>2</sub>  $\rightarrow$  S<sub>1</sub> relaxation between flashes. Samples received a maximum of 30 flashes. No artificial acceptors were added. Oxygen flash yield measurements were performed on a Joliot type electrode.<sup>13</sup> EPR monitoring<sup>12c</sup> showed little ( $\sim 5\%$ ) turnover of cyt b559, which remained always essentially oxidized and low spin.

Figure 1A shows the flash induced absorbance change ( $\lambda = 820$  nm) on turnover of core particles from the S<sub>1</sub> to S<sub>2</sub> states. The transient exhibits a single-exponential decay with  $t_{1/2} \sim 50 \pm 2$  s. By comparison, Figure 1B shows the S<sub>2</sub>  $\rightarrow$  S<sub>1</sub> relaxation measured by oxygen flash yield experiments at the same temperature on the Joliot electrode.<sup>13</sup> This was also essentially a single-exponential decay, with  $t_{1/2} \sim 65 \pm 5$  s. The two processes thus have comparable kinetics<sup>14</sup> and are consistent with the predominantly single-exponential S<sub>2</sub>  $\rightarrow$  S<sub>1</sub> relaxation behavior in

(9) Stranger, R.; Dubicki, L.; Krausz, E. *Inorg. Chem.* **1996**, *35*, 1041–1042.

(10) Kurreck, J.; Seeliger, A. G.; Reifarth, F.; Karge, M.; Renger, G. *Biochemistry* **1995**, *34*, 15721–15731.

(11) PS II membrane fragments were prepared according to ref 11a. Preparation of core complexes followed van Leeuwen et al. (ref 11b), incorporating perfusion chromatography (ref 11c) using a Poros HQ anion exchange column. (a) Berthold, D. A.; Babcock, G. T.; Yocum, C. F. *FEBS Lett.* **1981**, *134*, 231–234. (b) van Leeuwen, P. J.; Nieveen, M. C.; Meent, E. J.; Dekker, J. P.; van Gorkom, H. J. *Photosynth. Res.* **1991**, *28*, 149–153. (c) Roobol-Bóza, M.; Anderson, B. *Anal. Biochem.* **1996**, *235*, 127–133.

(12) See Supporting Information (refs 12a–d).

(13) Messinger, J.; Seaton, G.; Wydrzynski, T.; Wacker, U.; Renger, G. *Biochemistry* **1997**, *36*, 6862–6873.

<sup>‡</sup> Department of Chemistry.

<sup>§</sup> Research School of Chemistry.

<sup>||</sup> Research School of Biological Sciences.

(1) Abbreviations used: PS II, Photosystem II; OEC, Oxygen Evolving Complex; EXAFS, extended X-ray absorption fine structure; NIR, near infrared; EPR, electron paramagnetic resonance; Nd:YAG, neodymium-yttrium aluminium garnet; chl, chlorophyll; MCD, magnetic circular dichroism; FPLC, Fast Performance Liquid Chromatography.

(2) Debus, R. J. *Biochim. Biophys. Acta* **1992**, *1102*, 269–352.

(3) Yachandra, V. K.; Sauer, K.; Klein, M. P. *Chem. Rev.* **1996**, *96*, 2927–2950.

(4) Smith, P. J.; Pace, R. J. *Biochim. Biophys. Acta* **1996**, *1275*, 213–220.

(5) (a) Dingle, R. *Acta Chem. Scand.* **1966**, *20*, 33–44. (b) Ferguson, J. *Prog. Inorg. Chem.* **1970**, *12*, 159–293. (c) Davis, T. S.; Fackler, J. P.; Weeks, M. J. *Inorg. Chem.* **1968**, *7*, 1994–2002. (d) Sheats, J. E.; Czernuszewicz, R. S.; Dismukes, G. C.; Rheingold, A. L.; Petrouleas, V.; Stubbe, J.-A.; Armstrong, W. H.; Beer, R. H.; Lippard, S. J. *J. Am. Chem. Soc.* **1987**, *109*, 1435–1444. (e) Gamelin, D. R.; Kirk, M. L.; Stemmler, T. L.; Pal, S.; Armstrong, W. H.; Penner-Hahn, J. E.; Solomon, E. I. *J. Am. Chem. Soc.* **1994**, *116*, 2392–2399. (f) Brunold, T. C.; Gamelin, D. R.; Stemmler, T. L.; Mandal, S. K.; Armstrong, W. H.; Penner-Hahn, J. E.; Solomon, E. I. *J. Am. Chem. Soc.* **1998**, *120*, 8724–8738.

(6) Dismukes, G. C.; Mathis, P. *FEBS Lett.* **1984**, *178*, 51–54.

(7) Velthuys, B. R. *Biochim. Biophys. Acta* **1988**, *933*, 249–257.

(8) (a) Boussac, A.; Girerd, J.-J.; Rutherford, A. W. *Biochemistry* **1996**, *35*, 6984–6989. (b) Boussac, A. *J. Biol. Inorg. Chem.* **1997**, *2*, 580–585. (c) Boussac, A.; Un, S.; Horner, O.; Rutherford, A. W. *Biochemistry* **1998**, *37*, 4001–4007. (d) Horner, O.; Rivière, E.; Blondin, G.; Un, S.; Rutherford, A. W.; Girerd, J.-J.; Boussac, A. *J. Am. Chem. Soc.* **1998**, *120*, 7924–7928.

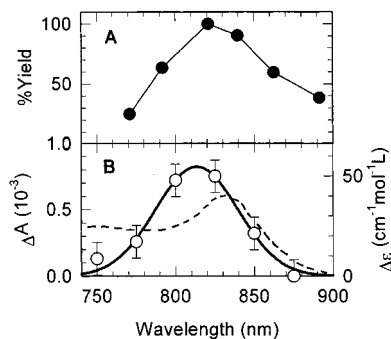


**Figure 2.** (A) Action spectrum for NIR induced multiline  $\rightarrow$   $g$  4.1 signal conversion at 150 K in PS II particles. Data points were taken from Boussac et al. (8a), Figure 3. Points were joined by linear segments. (B) Wavelength dependence of the NIR signal transient amplitude observed here in PS II core complexes for  $S_1 \rightarrow S_2$  turnover. Other conditions as in Figure 1A. Molar extinction scale assumes 70 chl/OEC (see text). The solid curve through the points is a Gaussian fit ( $\nu_{\max} \sim 12\,300\text{ cm}^{-1}$ ,  $\delta\nu_{1/2} \sim 1000\text{ cm}^{-1}$ ). The dashed curve is the expected contribution from a chl cation radical in  $\sim 1\%$  of centers (ref 18).

thylakoids at these temperatures.<sup>15</sup> Measurements of the absorption transient amplitude over a range of wavelengths are given in Figure 2B. The error shown is the standard deviation of the measurement (at 875 nm, but wavelength independent). In Figure 2A we reproduce the action spectrum for the NIR induced interconversion of the  $S_2$  state multiline to  $g$  4.1 signals from ref 8a. It is well-known that the presence of small alcohols (MeOH, EtOH, ethylene glycol) affects the balance between these two forms of the  $S_2$  state, favoring the multiline type. Figure 1C shows that MeOH (at 2% in buffer) does not interfere with and possibly enhances ( $\sim 30\%$ ) the NIR transient amplitude, while hydroxylamine extinguishes the signal, consistent with its known role in destabilizing the Mn cluster.<sup>2</sup> Figure 2 shows that the  $S_2 \rightarrow S_1$  transient absorption difference spectrum and the action spectrum for the low-temperature, NIR induced multiline to 4.1 conversion are very similar. On the basis of their activity and the chlorophyll  $a/b$  ratio, the core particles used here contain 50–70 chlorophylls per OEC. The molar extinction scale in Figure 2B assumes 70. Hence  $\epsilon_{\max}$  for the observed NIR band at 820 nm is  $\sim 35\text{--}60\text{ M}^{-1}\text{ cm}^{-1}$ . The band is sufficiently weak that it would have been difficult to detect in the earlier experiments,<sup>6,7</sup> which were probably dominated by a real,  $S_2$  state dependent chlorophyll band shift effect.<sup>12b</sup> Little interference from chl<sup>+</sup> radicals is evident in Figure 2B, as is expected on kinetic grounds under our conditions.

It has been proposed that the NIR transition responsible for the observed spin state changes in the OEC is due to an intervalence charge transfer in a MnIII–MnIV dimer component, or a high- to low-spin conversion in a MnIII (analogous to FeII systems).<sup>8d</sup> However, spin crossover is rare in MnIII<sup>16</sup> and has so far been observed only in strong (all nitrogen) ligand field environments. Further, Gamelin et al.<sup>5c</sup> have recently shown from MCD studies on MnIII–MnIV dimers that the weak NIR bands around  $10\,000\text{--}12\,000\text{ cm}^{-1}$  in such compounds are not intervalence bands, but arise from spin allowed d–d transitions within the Jahn–Teller split  $e_g$  levels of the MnIII ion. Such bands, with this assignment, are in fact well documented in monomeric and dimeric MnIII complexes.<sup>5</sup> Dingle has studied NIR bands in a number of 6-coordinate MnIII compounds.<sup>5a</sup> We have noticed an interesting correlation in his data, for complexes with predominantly O(N) ligation,<sup>12d</sup> between band intensity and position. This is shown in Figure 3. As the NIR band position increases in energy

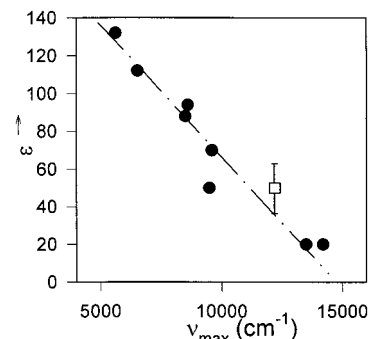


**Figure 3.** Closed points: Plot of band position ( $\nu_{\max}$ ) versus  $\epsilon$  for the d–d NIR band (see text) in a series of 6-coordinate monomeric MnIII complexes with predominantly O,N ligation (from Dingle (refs 5a and 12d)). The dashed line is a linear regression through these points. The open symbol is for the PS II band from Figure 2B, with the uncertainty range as discussed in the text.

from  $\sim 5000$  to  $15\,000\text{ cm}^{-1}$ , the intensity drops almost linearly. The OEC band identified here lies close to this correlation, which at present remains empirical.<sup>12d</sup>

Identification of the NIR band in PS II as a *spin allowed* d–d transition in a single MnIII ion has several implications for the Mn organization within the OEC, and the nature of the NIR induced EPR signal interconversion: (i) Since the  $S_1$  state contains no MnII,<sup>3</sup> the band is present in a MnIII ion that does not undergo oxidation on  $S_1 \rightarrow S_2$ , but rather alters its *ligand environment* on forming the  $S_2$  multiline state (i.e., “tuning” the  $e_g$  level split to bring the band into view). (ii) This MnIII is probably 6-coordinate, 5-coordinate MnIII (as in Mn catalase or superoxide dismutase) normally has too large an  $e_g$  level split for the band to be detectable (see ref 5f, but 5 coordination in a trigonal system of weak axial ligation might be possible). (iii) Since the formal MnIII spin state does not change but the NIR induced EPR interconversion may be thermally trapped, the likely mechanism for the latter is an electron transfer within components of the OEC, involving the d–d excited state generated continuously under illumination. This could involve oxidation of the MnIII (effectively equivalent to a Mn<sup>•••</sup>Mn charge transfer) or reduction of a species (ligand?) near the MnIII (eliminating the multiline), leading to oxidation of some other component which then generates the  $g$  4.1 signal (as in ref 4). However the process in the OEC appears to be without direct model compound precedent.

Boussac<sup>8b</sup> has shown that, as conventionally prepared, the multiline state of the OEC is usually heterogeneous, with two slightly different multiline forms being present and only one of these sensitive to the NIR induced multiline  $\rightarrow$  4.1 conversion (the “wing broadened” form). Interestingly, these two multiline types (“wing narrow”/“broad”) have been previously identified in another context,<sup>17</sup> the “broader” species being that stabilized by alcohols and proposed by us to arise from a bridge deprotonated state of a Mn dimer.<sup>4</sup> The result in Figure 1C that MeOH, if anything, enhances the  $S_2$  state NIR band is then totally consistent with this phenomenology. However, a definitive identification of the nature of the NIR band in PS II must await a detailed MCD study of the transition. Such experiments are currently planned in our laboratories.

**Acknowledgment.** We thank K. Jackman, W. Hillier, and D. Kuzek for valuable technical assistance and advice. This work was supported by the Australian Research Council.

**Supporting Information Available:** Experimental details, including graphs of NIR absorption characteristics and EPR spectra (PDF). This material is available free of charge via the Internet at <http://pubs.acs.org>.

JA9838662

(17) Smith, P. J.; Åhrling, K. A.; Pace, R. J. *J. Chem. Soc., Faraday Trans.* **1993**, *89*, 2863–2868.

(18) Davis, M. S.; Forman, A.; Fajer, J. *Proc. Natl. Acad. Sci. U.S.A.* **1979**, *76*, 4170–4174.

(14) Standard errors for  $t_{1/2}$  values in Figure 1 are for curve fitting to data sets shown. Intersample variation in these parameters is  $\sim 25\text{--}30\%$ .

(15) Messinger, J.; Schröder, W. P.; Renger, G. *Biochemistry* **1993**, *32*, 7658–7668.

(16) (a) Kaustov, L.; Tal, M. E.; Shames, A. I.; Gross, Z. *Inorg. Chem.* **1997**, *36*, 3503–3511. (b) Sim, P. G.; Sinn, E. *J. Am. Chem. Soc.* **1981**, *103*, 241–243.